Reaction Chemistry & Engineering

ROYAL SOCIETY OF CHEMISTRY

PAPER

View Article Online
View Journal

Cite this: DOI: 10.1039/d5re00539f

Emulsion droplet-enabled selective electrochemical oxidation of alcohols at industrially relevant current densities

Menglu Cai, [a] Shenyuan Gao,[a] Haoqiong Zhu,[a] Xiaozhong Wang,[ab] Gang Xu *[a] and Liyan Dai *[ab]

Received 5th December 2025,
Accepted 1st March 2026

DOI: 10.1039/d5re00539f

rsc.li/reaction-engineering

Selective oxidation plays a pivotal role in the interconversion of organic compounds and the synthesis of high-value products. However, industrial-scale electrochemical oxidation is often hindered by low reaction efficiency, limited current density, and excessive electrolyte waste. Herein, we reported a highly efficient one-pot emulsion-based electrochemical approach for aldehyde synthesis using catalytic amounts of TEMPO with sodium chloride and sodium bromide as electrolytes in a biphasic solvent system. This method achieves benzaldehyde in excellent yields (80–99%) with high Faraday efficiencies (76.4–90.9%) at 100–900 mA cm^{-2} current densities and tolerates substrate concentrations up to 4 mol L^{-1}. Gram-scale electrolysis of benzaldehyde at 2 A for 21.3 min produced 1.16 g of benzaldehyde with a 90.9% isolated yield and a production rate of 816.9 g m^{-2} h^{-1}. Furthermore, the method features recyclable electrolytes, reusable immobilized TEMPO, a representative substrate scope, and gram-scale synthesis, demonstrating both robustness and generality of the emulsion strategy, emphasizing its promise for industrial implementation.

1 Introduction

Organic electrosynthesis provides a sustainable alternative to traditional organic synthesis and has increasingly emerged as a promising approach for chemical transformations. In particular, for the production of high value-added fine chemicals and pharmaceutical intermediates that require conversion under mild conditions, electrochemical methods offer a superior and environmentally friendly synthetic pathway.[1–4] However, the practical applicability of the electrochemical methods remains a subject of debate,[5] as most reported electrosynthesis systems operate at relatively low current densities, typically in a double-digit or even single-digit milliamperes per square centimeter range.[6,7] Meanwhile, improving mass transfer efficiency, reducing ohmic resistance, and enhancing the selectivity of target products have also become key challenges in large-scale electrochemical production.[8,9] Low substrate concentrations and excessive solvent consumption in these systems result in high raw material costs and considerable energy demand during product separation, thereby undermining the economic viability of large-scale electrochemical production. For instance, the electrochemical oxidation of primary and secondary alcohols into their corresponding carbonyl compounds is a fundamental transformation in the synthesis of fragrances, pharmaceuticals and food additives.[10,11] Due to the high reactivity of aldehydes relative to their parent alcohols, overoxidation and competing side reactions are often inevitable during the process.[12] Therefore, precisely designing and controlling the selective oxidation process to achieve efficient conversion of primary raw materials into high-value-added products remain a central pursuit for researchers.

2,2,6,6-Tetramethylpiperidine-*N*-oxyl (TEMPO), which has gained widespread attention in both academic and industrial fields, is extensively employed for the selective oxidation of alcohols to aldehydes and ketones.[13,14] However, its high price and homogeneous nature have hindered its application in large-scale industry processes. Consequently, designing recyclable and reusable TEMPO-based systems while preserving high catalytic activity and selectivity continues to represent a significant challenge in the field of electrochemical oxidation. In recent years, numerous progress has been achieved in the immobilization of TEMPO and its derivatives on various supports, including mesoporous silica,[15,16] magnetic nanoparticles,[17] carbon nanotubes,[18] ionic liquids,[19] and so on. Moreover, the

[a] Zhejiang Provincial Key Laboratory of Advanced Chemical Engineering Manufacture Technology, College of Chemical and Biological Engineering, Zhejiang University, Hangzhou 310027, People's Republic of China.
E-mail: xugang_1030@zju.edu.cn
[b] Institute of Zhejiang University – Quzhou, 78 Jiuhua Boulevard North, Quzhou 324000, PR China. E-mail: dailiyan@zju.edu.cn

cooperative action of TEMPO with sodium hypochlorite (NaOCl) and sodium bromide has been shown to significantly improve the oxidation of alcohols to aldehydes as well.[14,20] Mo *et al.* achieved the continuous production of benzaldehyde by immobilizing TEMPO in a fixed-bed reactor, attaining a space–time yield (STY) of 516.95 kg m^{-3} h^{-1} with an alcohol conversion exceeding 90% and an aldehyde selectivity approaching 100%.[11] Similarly, Baumann *et al.* developed a robust metal-free process for the selective oxidation of alcohol using catalytic amounts of TEMPO in combination with NaBr/NaOCl as a co-oxidant, achieving over 90% yield of phenylpropanal and demonstrating the feasibility of scale-up.[21] Despite recent advances in heterogeneous TEMPO-catalyzed selective aldehyde synthesis, the development of practical and sustainable methods that allow for facile product separation and maintain high efficiency at industrially relevant current densities remains highly desirable.

Considering product separation and energy consumption, biphasic systems allow the spontaneous phase separation of organic and aqueous phases upon standing, thereby eliminating the need for cumbersome extraction steps.[22–27] For example, Zhang *et al.* developed a "sandwich-type" organic–solid–water (OSW) electrochemical system. By employing a Janus superwetting electrode to separate the organic and aqueous phases at the OSW interface, they achieved high selective oxidation of benzyl alcohol to benzaldehyde, as well as the direct electrosynthesis of high-purity benzaldehyde (91.7%) from concentrated benzyl alcohol without the need for a separation operation. This strategy provides a universal platform for the electrosynthesis of organic compounds that are insoluble in aqueous phases.[27] Organic syntheses involving immiscible liquid organic reagents, such as Pickering emulsions, have been also extensively studied because they can markedly enhance the interfacial reaction kinetics.[28,29] For example, Yang *et al.* designed a Pickering emulsion reaction system to accelerate the electrosynthesis of cyclohexanone oxime from cyclohexanone and nitrogen oxides. The emulsion droplets in this system acted as microreactors, and achieved a Faraday efficiency (FE) of 83.8% and a production rate of 0.78 mmol h^{-1} cm^{-2}, demonstrating significant advantages in reaction efficiency, selectivity, and environmental friendliness compared with conventional electrocatalytic strategies, while also highlighting the enhanced mass-transfer capabilities of the microemulsion system.[30]

Here, we report the construction of an emulsion system for selective electrochemical oxidation (Scheme 1). Leveraging the advantages of multiphase reactions and Pickering emulsion, the organic and aqueous phases undergo spontaneous separation upon standing, facilitating the efficient reuse of the saline aqueous phase. To achieve this goal, we developed a one-pot system enabling the *in situ* generation of hypohalous acid alongside TEMPO-mediated co-catalytic oxidation of alcohols. Under high-speed stirring (600 rpm), the generated hypohalous acid was efficiently in contact with both the substrate alcohol and TEMPO, affording aldehyde yields of 80–99% at industrially relevant current densities (100–900 mA cm^{-2}) and the overall Faraday efficiency (FE) exceeding 70%. Meanwhile, the combination of commercially available electrodes, compatibility with high-concentration substrates (4 M), and the robust cycling stability of both the electrolyte and immobilized TEMPO highlights the system's strong potential for industrial application.

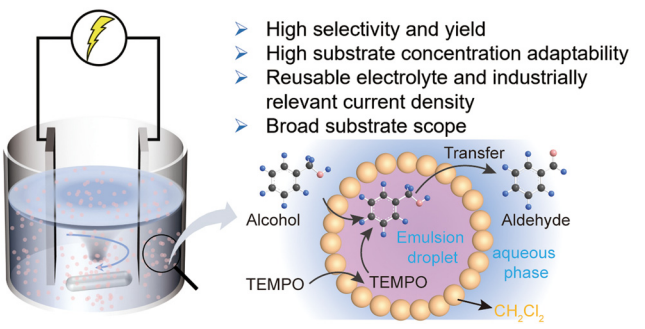

Scheme 1 Proposed strategy for selective electrochemical oxidation of alcohols.

2 Results and discussion

2.1 Electrochemical emulsion reaction strategy for alcohol oxidation

The key to achieving highly selective electrochemical oxidation of alcohol in a biphasic system lies in establishing efficient contact between the substrate and the oxidant. To investigate the influence of the water–oil emulsion on mass transfer, the electrochemical oxidation of benzyl alcohol to benzaldehyde was selected as a model reaction. Emulsion formation can be facilitated by rapid mechanical stirring, ultrasonication, or the introduction of surfactants, which collectively increases the interfacial area between the two phases and enhances mass transfer efficiency in biphasic reactions.[31–33] However, maintaining uniform dispersion of oil droplets in an aqueous phase by ultrasonication is challenging, and the use of surfactants may affect the electrochemical process. Hence, vigorous stirring was adopted as the optimal strategy for emulsion generation and maintenance. This method facilitated through mixing of aqueous and organic phases, producing numerous microdroplets, which can promote the efficient interphase mass transfer and consequently enhance the selectivity of the target reaction.[30] Organic solvents were first screened, and the results showed that dichloromethane (CH_2Cl_2) afforded a higher benzaldehyde yield while requiring a lower reaction voltage (Fig. S11) compared with ethyl acetate (EA), chloroform and toluene. Therefore, dichloromethane was selected as the preferred organic phase for the emulsion reaction in subsequent studies.

The NaClO–NaBr–TEMPO system has been extensively utilized for selective alcohol oxidation,[11,20,21] and numerous

studies have demonstrated that halide ions can serve as effective redox mediators (X^-/XO^-), highlighting the great potential of adapting this chemical strategy into an electrochemical platform.[3,34–36] Many of these systems enabled the oxidation of halide ions to higher valence states at high current densities, offering an efficient pathway for electrochemical conversion of alcohols to aldehydes under industrially relevant conditions. On the basis of previous studies,[3,21,30] we proposed that Cl^- can be oxidized to the active chlorine species, which synergistically cooperated with TEMPO and active bromine under vigorous stirring. The emulsion system enables rapid interfacial contact between the alcohol- and TEMPO-containing organic phase and the hypohalous acids generated in the aqueous phase, effectively suppressing direct electrode oxidation and overoxidation, thereby achieving highly selective conversion of alcohols to their corresponding aldehydes (Fig. 1a).

To validate the proposed strategy, the optimal anode material for the chlorine/bromide oxidation reaction was identified, and various electrode materials were investigated using linear scanning voltammetry (LSV) (Fig. S12). The DSA electrode has the lowest onset potential and the largest current density for the chlorine/bromide oxidation reaction. In bulk electrolysis, DSA also showed the best performance for benzyl alcohol oxidation (Fig. 1b). Thus, DSA was selected as the optimal anode for the following studies. Then, we utilized unsupported TEMPO in a one-pot undivided cell and examined the influence of the stirring rate on mass transfer, benzaldehyde yield, and the Faraday efficiency. Without stirring, the benzyl alcohol conversion was only 11.2% (Fig. 1c), as the oxidizing species generated in the aqueous phase are confined to the water–CH_2Cl_2 interface. The limited interfacial area and slow interphase diffusion significantly hinder mass transfer, which was lowering the reaction efficiency.[37] Additionally, under these conditions, substantial accumulation of active chloride occurred in the aqueous phase, and some active chloride is reduced at the cathode without any cathode suppressing method, leading to a decreased Faraday efficiency.[34] At stirring speeds of 200 rpm and 400 rpm, benzyl alcohol conversions exceeded 99%,

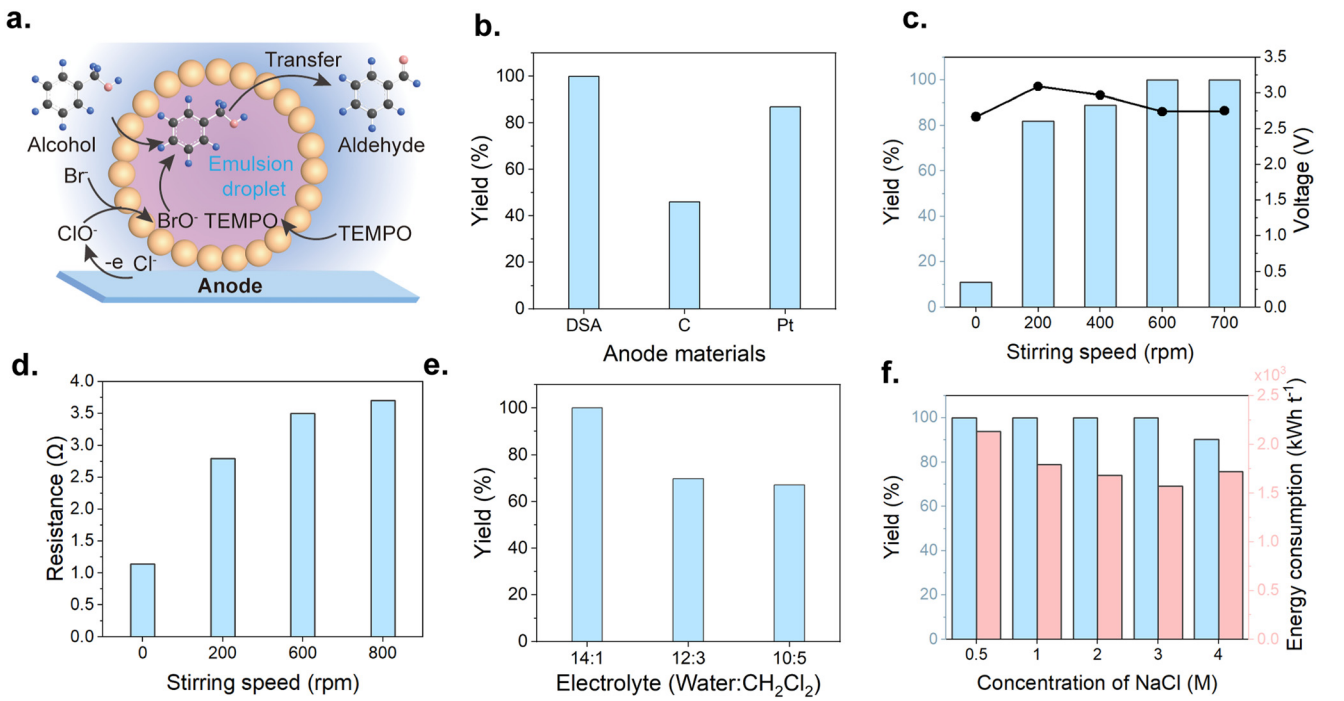

Fig. 1 Construction of the electrochemical emulsion reaction strategy in this work. a) The Pickering emulsion electrocatalytic aldehyde production route presented in this work. b) Effects of anode materials on benzaldehyde yield. The materials including dimensionally stable anode (DSA), carbon paper (CP) and platinum plate were investigated. The reaction was performed with 0.5 mmol of benzyl alcohol in 1 mL CH_2Cl_2 with 5 mol% TEMPO (4 mg), then adding 14 mL water with 3 M NaCl and 0.01 M NaBr. The current density is 100 mA cm^{-2} and the total charge passed is 2.2 F mol^{-1}. c and d) Effects of stirring speed on the yield of benzaldehyde, voltage and the solution resistance. Reaction conditions: 0.5 mmol of benzyl alcohol in 1 mL CH_2Cl_2 with 5 mol% TEMPO (4 mg), then adding 14 mL water with 3 M NaCl and 0.01 M NaBr at different stirring speeds. Anode: DSA (1 cm^2). Cathode: nickel foam (1 cm^2). The current density is 100 mA cm^{-2} and the total charge passed is 2.2 F mol^{-1}. The reaction voltage was measured prior to the end of the experiment. The solution resistance value was obtained from electrochemical impedance spectroscopy (EIS). e) Effects of the organic phase ratio on benzaldehyde yield. Reaction conditions: 0.5 mmol of benzyl alcohol with 5 mol% TEMPO (4 mg). Anode: DSA (1 cm^2). Cathode: nickel foam (1 cm^2). The current density is 100 mA cm^{-2} and the total charge passed is 2.2 F mol^{-1}. f) Changes in benzaldehyde yield and system energy consumption at different NaCl concentrations. In a dual *Y*-axis chart, the bar colours represent the descriptions of the corresponding colour axes. Reaction conditions: 0.5 mmol of benzyl alcohol in 1 mL CH_2Cl_2 with 5 mol% TEMPO (4 mg), then adding 14 mL water with various concentrations of NaCl and 0.01 M NaBr. Anode: DSA (1 cm^2). Cathode: nickel foam (1 cm^2). Stirring at 600 rpm. The current density is 100 mA cm^{-2} and the total charge passed is 2.2 F mol^{-1}.

while benzaldehyde yields were only 82.1% and 88.9%, respectively. At lower stirring speed, although small droplets disperse into the aqueous phase, the two-phase electrolyte remained well-defined (Fig. S13).

Droplet adhesion on electrodes led to increased cell voltage (3.09 V and 2.97 V) and pronounced voltage fluctuations as we observed (Fig. 1c and S13). To further explore the impact of stirring, solution resistance was measured at various stirring rates (Fig. 1d). And the results showed that uniform droplets formed at 600 rpm and 800 rpm corresponding to similar resistance values, indicating improved interfacial contact. When the stirring speed exceeded 600 rpm, reaction performance improved markedly, with both benzyl alcohol conversion and benzaldehyde selectivity exceeding 99% (Fig. S14 and S15). Under these conditions, the electrolyte formed a uniform dispersion with no distinct phase interface (Fig. S13), and the cell voltage stabilized at 2.7–2.8 V, slightly higher than that observed for pure aqueous electrolysis. These observations indicated that vigorous stirring enhances interfacial mass transfer, allowing the electrode reaction to proceed predominantly *via* the chlorine evolution reaction, with minimal influence from the organic phase.[38–40]

The organic solvent proportion in the biphasic system strongly influenced reaction performance (Fig. 1e). Increasing the organic-phase content increased the solution resistance (Fig. S16), likely due to more oil droplets adhering to the electrode surface. Furthermore, a higher organic-phase content reduced the dispersion of the organic phase in water, weakening interfacial mass transfer and resulting in direct oxidation of alcohols and aldehydes, which produced some overoxidized by-products.[41] A larger proportion of organic solvent also promoted direct dissolution of Cl_2 or Br_2 into CH_2Cl_2, preventing their conversion into the more reactive hypohalous acid (Fig. S17 and S18). Overall, optimization of the stirring rate and electrolyte composition facilitates efficient *in situ* generation of hypohalous acid in the NaCl–NaBr–TEMPO system, enabling efficient contact between the substrate and the oxidant produced *in situ*, thus achieving highly selective and high-yield preparation of aldehydes. This is because vigorous stirring converts the continuous organic phase into uniformly dispersed droplets, forming an oil-in-water (O/W) emulsion, and the resulting emulsion increases the interfacial area while maintaining good conductivity, thereby enhancing mass transfer and facilitating selective oxidation.[42]

To elucidate the role of each component in the NaCl–NaBr–TEMPO system, we then investigated how variations in electrolyte composition influence the selective oxidation of benzyl alcohol to benzaldehyde (Fig. S9 and Table S1). In the absence of TEMPO, the benzaldehyde yield fell to 24%, and it further decreased to 9.2% when NaBr was removed (Table S1, entries 4 and 5), demonstrating that TEMPO is vital for catalysis, and the bromine redox process is a key step facilitated by chlorine and TEMPO. This is because without the bromine redox process, the active chlorine generated at the anode exhibited insufficient oxidative ability to directly oxidize benzyl alcohol or to convert TEMPO into the [R–N^+ = O] active species required for substrate oxidation.[43] When NaBr–TEMPO or NaBr was used alone as the reaction medium, the benzaldehyde yields were 85.0% and 64.4%, with the corresponding FEs of 70.8% and 53.7% (Table S1, entries 2 and 3). Bromine species ($Br^{\bullet}$ or Br^+) are less effective than NaClO in regenerating TEMPO from TEMPOH according to previous study.[44] Hence, bromine and TEMPO act synergistically as co-catalysts, ensuring both the stability and efficiency of the catalytic cycle (Table S1, entries 7 and 9). These findings demonstrated that the NaCl–NaBr–TEMPO two-phase system, with concentrated NaCl and catalytic amounts of NaBr and TEMPO, achieves efficient and highly selective electrooxidation of benzyl alcohol.

Acting as the primary conductive medium and participating in the anodic reaction, NaCl concentration critically influences both the reaction efficiency and energy consumption. Experiments with NaCl concentration from 0.5 M to 3 M showed that the benzaldehyde yield remains above 99%, while the energy consumption dropped from 2132.6 kWh t^{-1} to 1571.39 kWh t^{-1} (Fig. 1f, Note S2 and Fig. S19). These results demonstrated that the system performed efficiently across a wide concentration range, with 3 M NaCl identified as the optimal electrolyte concentration in terms of energy consumption.

2.2 TEMPO catalyst immobilization and characterization

Despite the system's excellent performance, with high selectivity, yield, Faraday efficiency, and industrially relevant current density, the high cost and homogeneous nature of TEMPO present major challenges for large-scale implementation. To address this limitation, a heterogeneous TEMPO catalyst was prepared by anchoring TEMPO onto the silica through reduction and amination reactions (Fig. 2a).[45,46] As detected by FT-IR (Fig. 2b and S20), TEMPO–silica showed characteristic absorption peaks corresponding to C–H stretching vibrations at 2991 cm^{-1} and 2942 cm^{-1}, and an additional peak at 1389 cm^{-1} attributed to the N–O radical stretching vibration,[11,47] closely matching the infrared features of the TEMPO monomer.[45] X-ray photoelectron spectroscopy (XPS) analysis revealed a clear N 1s signal (Fig. S21), and the deconvolution of the peak showed two nitrogen species, nitroxyl-N (N–O, 400.94 eV) and amino-N (C–N–C, 399.19 eV) (Fig. 2c), confirming that TEMPO was successfully grafted on the silica, in agreement with FT-IR results.

BTE characterization further confirmed the surface area and the porosity of silica and TEMPO–silica; both materials exhibit type IV isotherms with clear H_2 hysteresis loops (Fig. 2d) according to the IUPAC classification.[48] The saturated adsorption plateau appearing in the relative pressure range (P/P_0 of 0.5–0.99) indicates that both samples possess well-defined mesoporous structures (Fig. S22),[49,50] and the detailed textural parameters of the two samples are summarized in Table S2. TEMPO–silica shows a reduced

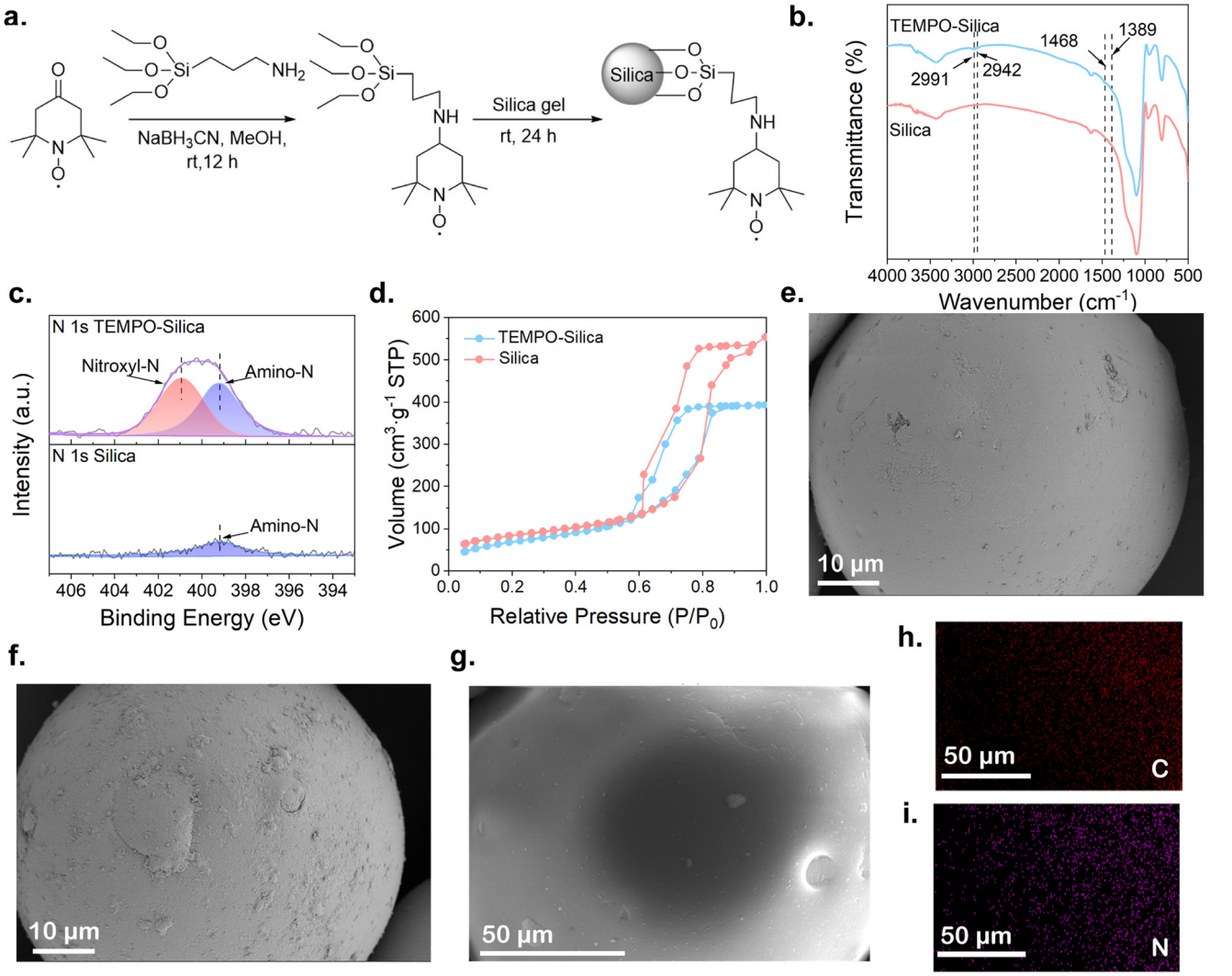

Fig. 2 Characterization of immobilized TEMPO–silica. a) Synthesis procedure for immobilizing TEMPO on silica. b) FT-IR spectra of silica and TEMPO–silica. c) The N 1s XPS spectra of silica and TEMPO–silica. d) N_2 adsorption–desorption isotherms of silica and TEMPO–silica. SEM images of e) silica and f) TEMPO–silica and the elemental mapping images g–i) of TEMPO–silica.

specific surface area, pore volume and average pore size, compared to pristine silica, indicating partial pore occupation by TEMPO moieties and the formation of a multi-level hierarchical mesoporous structure. The surface morphology of both samples was further examined by scanning electron microscopy (SEM). The pristine silica exhibited a spherical morphology with an average diameter of ~50 μm (Fig. S23a), while the TEMPO–silica sample displayed a rougher surface (Fig. 2f and S23b), likely resulting from the grafting of TEMPO *via* the APTES silane coupling agent. Elemental mapping by energy-dispersive X-ray spectroscopy (EDS) revealed a homogeneous distribution of C and N elements on the TEMPO–silica microsphere surface (Fig. 2g–i), in addition to the inherent Si and O elements from the silica matrix (Fig. S23g). And the overlapping spatial distributions of C and N further verified the uniform immobilization of TEMPO on the silica surface.

2.3 Practical application potential in emulsion-based aldehyde synthesis

After synthesizing the immobilized TEMPO–silica material, we investigated the electrochemical–chemical tandem alcohol oxidation reaction in a single-cell system. The catalytic performance of TEMPO–silica was first evaluated, revealing that its activity remained essentially unchanged after immobilization. This result indicates that the immobilized TEMPO catalyst can effectively replace the TEMPO monomer (Fig. 3a). Given that the TEMPO content in TEMPO–silica was approximately 1 wt% (Fig. S23g, calculated based on the N content), 40 mg of TEMPO–silica was initially added to assess its catalytic activity. Under these conditions, the yield of benzaldehyde exceeded 99%, with an overall Faraday efficiency of 90.9%, and the performance remained stable even when the catalyst dosage was reduced to 20 mg.

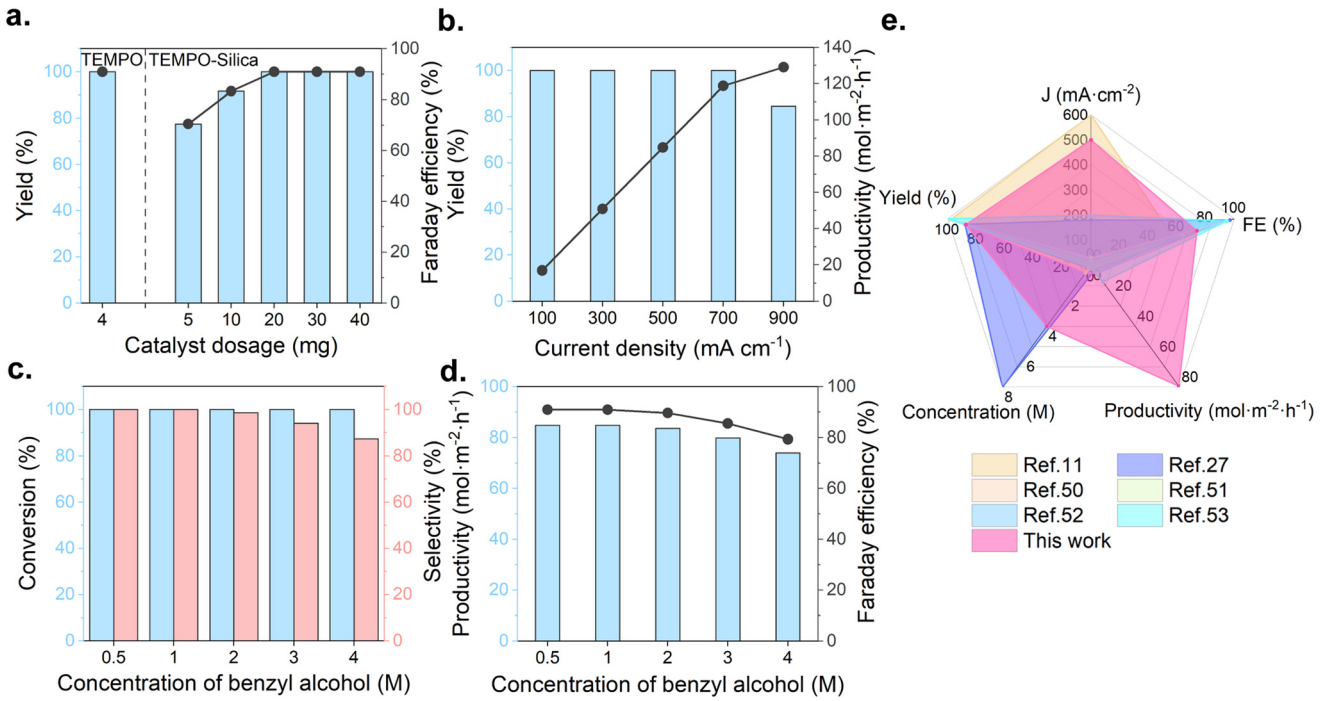

Fig. 3 The performance of benzaldehyde synthesis in an emulsion system. a) The effect of different TEMPO–silica dosages on the reaction performance. Reaction conditions: 0.5 mmol of benzyl alcohol in 1 mL CH_2Cl_2 with different catalyst dosages, then adding 14 mL water with 3 M NaCl and 0.01 M NaBr. Anode: DSA (1 cm^2). Cathode: nickel foam (1 cm^2). Stirring at 600 rpm. Total charge passed: 2.2 F mol^{-1}. b) The yield and productivity of benzaldehyde electrosynthesis under different current densities. Reaction conditions: 0.5 mmol of benzyl alcohol in 1 mL CH_2Cl_2 with 5 mol% TEMPO (4 mg), then adding 14 mL water with 3 M NaCl and 0.01 M NaBr. Anode: DSA (1 cm^2). Cathode: nickel foam (1 cm^2). Stirring at 600 rpm. Total charge passed: 2.2 F mol^{-1}. c and d) The effect of substrate concentration on reaction performance. The reaction conditions are the same as those in b) except for the substrate concentration and the current density (500 mA cm^{-2}). In a dual *Y*-axis chart, the bar colors represent the descriptions of the corresponding color axes. e) Comparison of current density, yield, FE, concentration of the substrate and productivity against the currently reported electrochemical synthesis for benzaldehyde.

Productivity is a critical parameter in industrial applications, and at comparable performance levels, higher current densities typically result in enhanced productivity and improved prospects for practical application. Remarkably, the electrolysis system achieved nearly 100% yield of benzaldehyde over a broad current density range (100–700 mA cm^{-2}, Fig. 3b), reaching a maximum productivity of up to 130 mol m^{-2} h^{-1}. With further increase of the current density, the selectivity declined, likely owing to the direct anodic oxidation of benzaldehyde and the formation of overoxidized by-products.[41]

Increasing the substrate concentration can effectively reduce solvent consumption, thereby lowering both production and separation costs. However, in electrochemical oxidation processes, substrate concentrations are typically limited due to direct electrode oxidation and overoxidation side reactions. To evaluate this effect, we examined various substrate concentrations in the CH_2Cl_2 phase at a current density of 500 mA cm^{-2}. The results revealed that the system exhibits excellent tolerance to high substrate concentrations, with the productivity reaching 80 mol m^2 h^{-1}, and the benzaldehyde yield exceeded 94% at concentrations below 3 mol L^{-1} and decreased modestly to 87.3% at 4 mol L^{-1} (Fig. 3c and d). The decline in selectivity at higher concentration was likely due to the increased benzaldehyde content in the organic phase, which promotes side reactions as mentioned above. Compared with the existing electrochemical oxidation studies of benzyl alcohol,[11,27,51–54] this two-phase reaction system enables efficient benzaldehyde synthesis under industrially relevant current densities and high substrate concentrations, demonstrating the outstanding productivity and promising potential for industrial application (Fig. 3e, Table S3).

2.4 Electrolyte recycling and the immobilized TEMPO recycling process

In industrial practice, the recycling of saline wastewater mainly relies on ion exchange, membrane separation and evaporation techniques.[55,56] However, conventional evaporation processes are highly energy-intensive, while both ion exchange and membrane separation require costly membranes. In the treatment of high-salinity wastewater, membrane durability is significantly reduced,[57,58] leading to increased maintenance cost. Although the feasibility of bromine recycling was explored in our previous study,[59] the process required secondary treatment involving the extraction of the saline phase and precipitation of the organic phase at

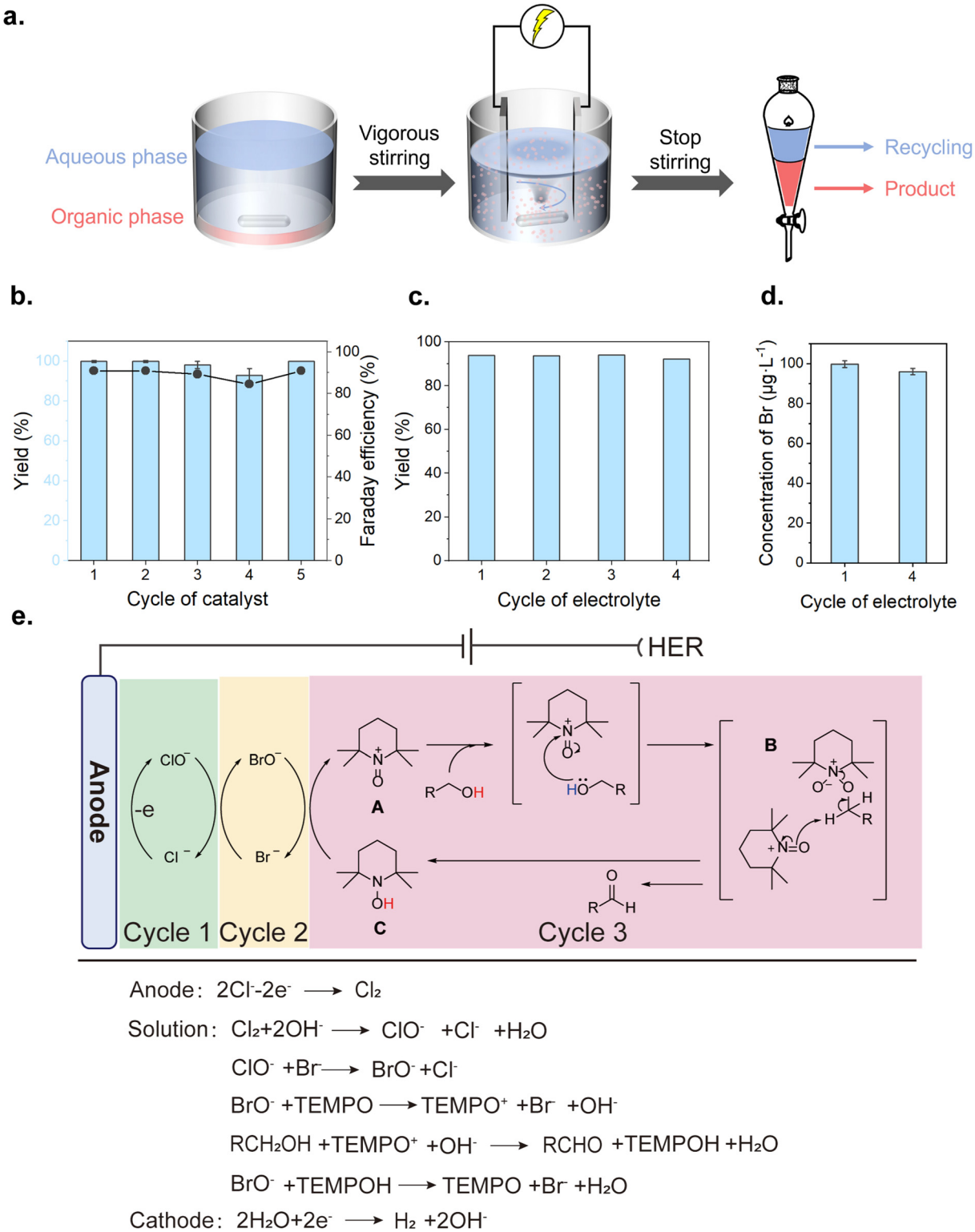

Anode: $2Cl^- - 2e^- \longrightarrow Cl_2$

Solution: $Cl_2 + 2OH^- \longrightarrow ClO^- + Cl^- + H_2O$

$ClO^- + Br^- \longrightarrow BrO^- + Cl^-$

$BrO^- + TEMPO \longrightarrow TEMPO^+ + Br^- + OH^-$

$RCH_2OH + TEMPO^+ + OH^- \longrightarrow RCHO + TEMPOH + H_2O$

$BrO^- + TEMPOH \longrightarrow TEMPO + Br^- + H_2O$

Cathode: $2H_2O + 2e^- \longrightarrow H_2 + 2OH^-$

Fig. 4 Electrolyte recycling and TEMPO–silica stability test. a) Reaction scheme for the electrochemical oxidation of benzyl alcohol and the recycling process. b) Yield and Faraday efficiency of benzaldehyde during the TEMPO–silica recycling process. Reaction conditions: benzyl alcohol (0.5 mmol) with initial TEMPO–silica (40 mg) in 1 mL CH_2Cl_2. Aqueous phase: 14 mL water with 3 M NaCl and 0.01 M NaBr. Anode: DSA (1 cm^2). Cathode: nickel foam (1 cm^2). Stirring at 600 rpm. Current density: 100 mA cm^{-2}. Total charge passed: 2.2 F mol^{-1}. All experiments employed recycled TEMPO–silica. In a dual *Y*-axis chart, the bar colours represent the descriptions of the corresponding colour axes. c) Yield of benzaldehyde during four recycles of aqueous solution. See SI for details. d) The concentration of bromine in aqueous solution after the first cycle and the fourth cycle, as determined using ICP-MS. e) The proposed mechanism of NaCl–NaBr–TEMPO-mediated electrooxidation of alcohol.

0 °C for 30 min to achieve the complete phase separation. In contrast, the current system operates as a two-phase reaction system. Vigorous stirring induces emulsification without adding additional amphiphilic agents, and upon completion, the organic and aqueous phases can be readily separated by simple standing, enabling straightforward electrolyte recovery and recycling (Fig. 4a).

For TEMPO–silica recycling (Note S1), after each reaction cycle, the catalyst was separated by filtration through a 0.22 μm microporous membrane and subsequently washed three times with deionized water and CH_2Cl_2, respectively. As shown in Fig. 4b, both the benzaldehyde yield and Faraday efficiency gradually decreased with an increasing cycle number, and declined to 93.0% and 84.5% by the fourth cycle. Due to the small size of the catalyst particles, repeated filtration and washing operations led to a recovery of only 35% of TEMPO–silica after four cycles, significantly lower than the optimal dosage as shown in Fig. 3a. Thus, three parallel experiments were conducted to further verify that the decrease in catalytic performance is primarily attributed to physical mass loss of the recovered catalyst rather than chemical deactivation or halogen leaching. The TEMPO–silica catalyst recovered after the fourth cycle was mixed evenly, and 20 mg was used for a fifth-cycle reaction (Fig. S24). The results showed that both the benzaldehyde yield and Faraday efficiency returned to their initial levels (Fig. 4a). Deactivation of the heterogeneous TEMPO catalysts has been reported to mainly originate from the gradual loss of active sites caused by continuous leaching of TEMPO moieties,[60] which is associated with the irreversible cleavage of the covalent C–N bonds.[61] Within the limited number of reuse experiments conducted, we therefore attribute the performance decline observed during the previous cycles to the physical catalyst loss rather than the intrinsic deactivation of the immobilized TEMPO sites.

To further examine the influence of TEMPO and halogen species, electrolyte recycling experiments and TEMPO–silica cycles were performed independently. After each electrolysis, the aqueous phase was recovered for reuse, with 20 mg of TEMPO–silica added for each subsequent cycle (Note S1). Over four consecutive electrolyte recycling runs without replenishing chloride or bromide ions, the benzaldehyde yield consistently exceeded 90%, accompanied by a slight voltage from 2.9 V to 3.2 V (Fig. 4c and S25). Meanwhile, the DSA anode still maintains its surface trench structure after undergoing TEMPO–silica and electrolyte cycle experiments (Fig. S26 and S27). These results further indicate that the yield decrease in the catalyst recycling test (Fig. 4b) mainly originated from catalyst loss rather than the electrolyte degradation and the DSA deactivation, demonstrating the robustness of this emulsion system. Given that the chloride concentration far exceeded the critical threshold, ICP-MS was further employed to monitor the bromide content during the first and fourth cycles. The bromide concentration and total amounts remained effectively unchanged, with variances of 1.76 and 1.55, respectively (Fig. 4d). These results demonstrate that both the halogen mediator and the immobilized catalyst can be effectively reused, supporting the system's potential for sustainable, large-scale electrooxidation.

2.5 Proposed reaction mechanism and the scope of electrochemical oxidation

As shown in Table S1, the presence of TEMPO and NaBr exerts a significant influence on the probe reaction. TEMPO is vital for catalysis, and the bromine redox process is a key step facilitated by chlorine and TEMPO. Based on previous studies, the alcohol oxidation catalyzed by TEMPO in the presence of sodium bromide and sodium hypochlorite proceeds through the following steps as presented in Fig. 4e: first, Cl^- undergoes oxidation *via* a two-electron process at the anode to generate hypochlorite (ClO^-),[3] which subsequently transfers electrons *via* the Br/TEMPO redox mediator to generate the oxidatively active species A $[R_2N^+{=}O]$.[21,44] The N–O radical in $[R_2N^+{=}O]$ attacks the hydroxyl group of the alcohol substrate, abstracting the hydrogen atom to form coupling intermediate B. Intermediate B then undergoes α-H elimination to yield the corresponding aldehyde product and the by-product TEMPOH. Finally, TEMPOH is re-oxidized by BrO^- to regenerate TEMPO, thereby completing the catalytic redox cycle.[62,63] At the cathode, the dominant reaction is the hydrogen evolution reaction (HER). This cathodic process generates hydroxide ions, which help maintain the alkaline environment required for stabilizing hypohalite species and do not directly participate in the oxidation of the organic substrate. To verify the proposed mechanism, a halide-free experiment was conducted to confirm the essential role of the halogen cycle. As shown in Fig. S28, benzaldehyde was scarcely produced under halogen-free conditions, which is consistent with the proposed pathway for the generation of oxidatively active species A.[11,44] An N_2-treated experiment was further conducted to exclude the influence of dissolved oxygen, and the yield of benzaldehyde in the solution pretreated with N_2 for 30 min was comparable to that obtained under conventional conditions. These results, together with the related control experiments (Fig. S29, Table S1), further confirm that hypohalous acids are generated *via* the anodic oxidation of halide ions to form halogens, which subsequently react with water,[3,11] rather than originating from dissolved oxygen. Moreover, they highlight the essential role of *in situ* hypohalite generation in the NaCl–NaBr–TEMPO system.

A variety of substrates were also examined to evaluate the generality of this system, including primary, secondary, and aromatic alcohols such as 4-pyridinemethanol, 2-thiophenemethanol, furfuryl alcohol, and vanillyl alcohol. Importantly, the oxidation products of vanillyl alcohol and heteroaromatic alcohols are widely used as fine-chemical building blocks or are closely related to intermediates encountered in pharmaceutical and functional-material

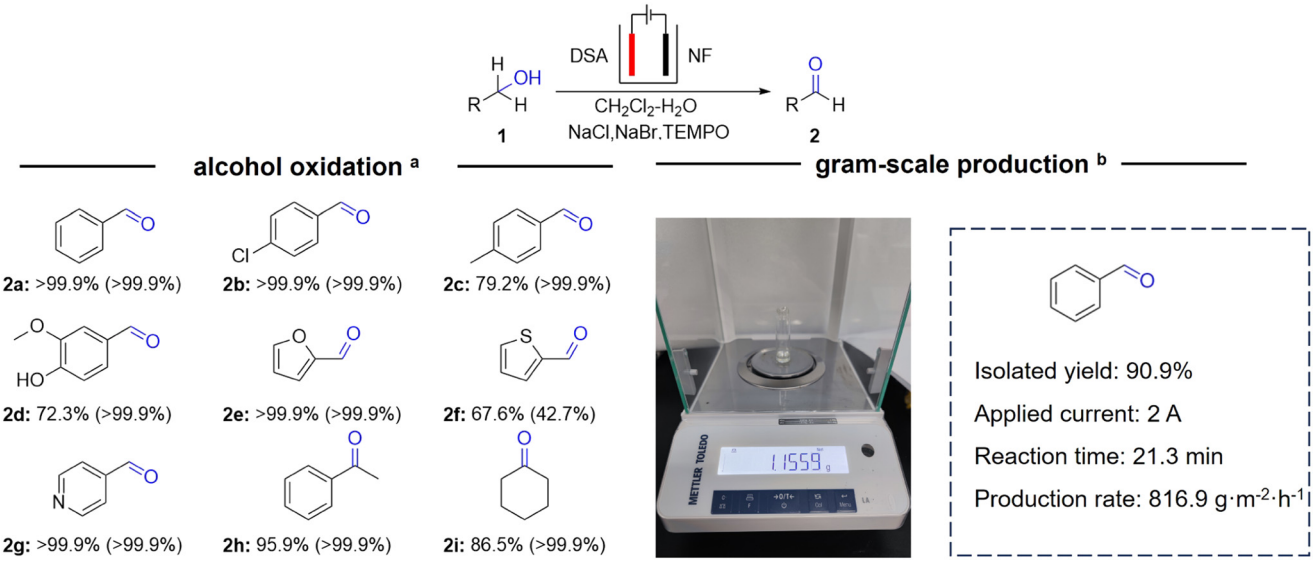

Scheme 2 Universality of the electrochemical oxidation for different alcohol substrates and the scaled-up production. [a]Reaction conditions: substrate (0.5 mmol) with initial TEMPO–silica (30 mg) in 1 mL CH_2Cl_2. Aqueous phase: 14 mL water with 3 M NaCl and 0.01 M NaBr. Anode: DSA (1 cm^2). Cathode: nickel foam (1 cm^2). Stirring at 600 rpm. Current density: 100 mA cm^{-2}. Total charge passed: 2.4 F mol^{-1}. The values directly displayed are the substrate conversion, and the values in brackets represent product selectivity. [b]For gram-scale production, 3 M of benzyl alcohol with 5 wt% TEMPO in 4 mL CH_2Cl_2. Aqueous phase: 56 mL water with 3 M NaCl and 0.01 M NaBr. The reaction was stirred at 600 rpm and 500 mA cm^{-2}. Total charge passed: 2.4 F mol^{-1}. Anode: DSA (4 cm^2). Cathode: nickel foam (4 cm^2).

synthesis.[10,64] The selected examples were chosen to represent different electronic and steric environments. Results showed that the system exhibited excellent aldehyde selectivity (>99%) in the oxidation of diverse substituted aromatic alcohols (Scheme 2, Fig. S30–S46). Primary alcohols achieved high conversion rates ranging from 79% to 99%. In contrast, for secondary alcohols, such as α-phenylethanol and cyclohexanol, although product selectivity remained high, the substrate conversions decreased to 95.9% and 86.5%, respectively, with a concomitant decrease in Faraday efficiency. This is likely attributed to the greater steric hindrance at β-C in secondary alcohols, which impedes the formation of the coupling intermediate B and the hydrogen abstraction process as discussed in the mechanism part.[44,62] Heteroatom-containing alcohols such as 4-methanolpyridine and furfuryl alcohol were also efficiently oxidized with good selectivity, whereas 2-thiophenemethanol exhibited a significantly lower selectivity (42.7%) due to the high reactivity of the thiophene ring, which promotes the formation of halogenated compounds (Fig. S41–S42). To illustrate its industrial applicability, benzaldehyde was produced on a gram scale at a constant current of 2 A for 21.3 min using a DSA anode (4 cm^2). Following standing and rotary evaporation, 1.16 g of benzaldehyde was successfully isolated, achieving a 90.9% yield and a production rate of 816.9 g m^{-2} h^{-1}. These results, together with the system's high performance across a broad current density range, underscore the versatility of the emulsion-based reaction strategy and highlight its potential for practical, large-scale electrochemical synthesis of aldehydes.

3 Conclusions

In this work, we developed a one-pot emulsion-based electrochemical system for highly selective alcohol oxidation, in which rapid stirring generates microdroplets without the need for external amphiphilic additives. Benefiting from the exceptional selectivity of TEMPO, the system achieved a benzaldehyde yield up to 99% with a Faraday efficiency of 90.9%. Combining the advantages of multiphase reactions and Pickering emulsion, the system enabled high benzaldehyde yields (80–99%) and Faraday efficiencies (76.4–90.9%) at industrially relevant current densities (100–900 mA cm^{-2}) and tolerated high substrate concentrations (up to 4 mol L^{-1}), which represented record-high performance among reported alcohol electrooxidation systems. The biphasic design facilitates easy phase separation and electrolyte recycling, while the immobilized TEMPO–silica maintains stable performance over multiple cycles. Moreover, the representative substrate scope and gram-scale applicability further demonstrated the compatibility and feasibility of this emulsion-based strategy for industrial applications. Combined with its varied substrate scope and gram-scale productivity, this emulsion-based system offers an economical and sustainable pathway for selective electrooxidation under practical conditions, providing a generalizable platform for scalable mediated electrosynthesis.

Author contributions

Menglu Cai: methodology, conceptualization, formal analysis, funding acquisition, investigation, writing – original draft,

writing – review & editing, and visualization. Shenyuan Gao: visualization and data curation. Haoqiong Zhu: formal analysis, visualization, investigation and data curation. Xiaozhong Wang: writing – review & editing, resources and data curation. Gang Xu: writing – review & editing and resources. Liyan Dai: writing – review & editing, supervision and resources.

Conflicts of interest

None of the authors has a conflict of interest to disclose.

Data availability

The data that support the findings of this study are available from the corresponding author upon reasonable request.

Error bars (where shown) in Fig. 4b and d show the spread of data observed in triplicate measurements, where independent samples were tested for each measurement. The data shown without error bars are from individual experimental measurements.

Supplementary information (SI) is available. See DOI: https://doi.org/10.1039/d5md01149c.

Acknowledgements

We acknowledge the China Postdoctoral Science Foundation (GZC20250765, 2022M722728) (M. C.) and the Zhejiang Provincial Natural Science Foundation of China (LMS26B060001) (M. C.) for providing support for this work.

References

1 Z.-W. Hou, D.-J. Liu, P. Xiong, X.-L. Lai, J. Song and H.-C. Xu, Site-Selective Electrochemical Benzylic C–H Amination, *Angew. Chem., Int. Ed.*, 2021, **60**, 2943–2947.

2 Y. Zhao, M. Duan, C. Deng, J. Yang, S. Yang, Y. Zhang, H. Sheng, Y. Li, C. Chen and J. Zhao, Br^-/BrO^--mediated highly efficient photoelectrochemical epoxidation of alkenes on α-Fe_2O_3, *Nat. Commun.*, 2023, **14**, 1943.

3 W. R. Leow, Y. Lum, A. Ozden, Y. Wang, D.-H. Nam, B. Chen, J. Wicks, T.-T. Zhuang, F. Li, D. Sinton and E. H. Sargent, Chloride-mediated selective electrosynthesis of ethylene and propylene oxides at high current density, *Science*, 2020, **368**, 1228–1233.

4 R. Wu, F. Li, X. Cui, Z. Li, C. Ma, H. Jiang, L. Zhang, Y. P. J. Zhang, T. Zhao, Y. Zhang, Y. Li, H. Chen and Z. Zhu, Enzymatic Electrosynthesis of Glycine from CO_2 and NH_3, *Angew. Chem., Int. Ed.*, 2023, **62**, e202218387.

5 D. Lehnherr and L. Chen, Overview of Recent Scale-Ups in Organic Electrosynthesis (2000–2023), *Org. Process Res. Dev.*, 2024, **28**, 338–366.

6 P. Xiong, H.-B. Zhao, X.-T. Fan, L.-H. Jie, H. Long, P. Xu, Z.-J. Liu, Z.-J. Wu, J. Cheng and H.-C. Xu, Site-selective electrooxidation of methylarenes to aromatic acetals, *Nat. Commun.*, 2020, **11**, 2706.

7 X. Fu, J. B. Pedersen, Y. Zhou, M. Saccoccio, S. Li, R. Sažinas, K. Li, S. Z. Andersen, A. Xu, N. H. Deissler, J. B. V. Mygind, C. Wei, J. Kibsgaard, P. C. K. Vesborg, J. K. Nørskov and I. Chorkendorff, Continuous-flow electrosynthesis of ammonia by nitrogen reduction and hydrogen oxidation, *Science*, 2023, **379**, 707–712.

8 N. Tanbouza, T. Ollevier and K. Lam, Bridging Lab and Industry with Flow Electrochemistry, *iScience*, 2020, **23**, 101720.

9 G. Laudadio, The Role of Synthetic Organic Electrochemistry in the Technological Revolution of Pharmaceutical Industry, *Chimia*, 2025, **79**, 417–423.

10 X. Pan, L. Sun, K. Chen, J. Zheng, S. Xu, C. Miao and G. Zhao, Optimization of competitive adsorption via oxygen vacancies on NiCo hydroxides for selective electrosynthesis of adipic acid coupled with hydrogen production, *EES Catal.*, 2025, **3**, 1345–1357.

11 T. Lin, M. Cai, H. Chen and Y. Mo, Selective electrosynthesis of aldehydes at industrially relevant current densities via tandem electrochemical–chemical catalysis, *Green Chem.*, 2024, **26**, 11290–11302.

12 N. Zhang, Y. Zou, L. Tao, W. Chen, L. Zhou, Z. Liu, B. Zhou, G. Huang, H. Lin and S. Wang, Electrochemical Oxidation of 5-Hydroxymethylfurfural on Nickel Nitride/Carbon Nanosheets: Reaction Pathway Determined by In Situ Sum Frequency Generation Vibrational Spectroscopy, *Angew. Chem., Int. Ed.*, 2019, **58**, 15895–15903.

13 M. Li, K. Klunder, E. Blumenthal, M. B. Prater, J. Lee, J. E. Matthiesen and S. D. Minteer, Ionic Liquid Stabilized 2,2,6,6-Tetramethylpiperidine 1-Oxyl Catalysis for Alcohol Oxidation, *ACS Sustainable Chem. Eng.*, 2020, **8**, 4489–4498.

14 H. A. Beejapur, Q. Zhang, K. Hu, L. Zhu, J. Wang and Z. Ye, TEMPO in Chemical Transformations: From Homogeneous to Heterogeneous, *ACS Catal.*, 2019, **9**, 2777–2830.

15 A. Machado, M. H. Casimiro, L. M. Ferreira, J. E. Castanheiro, A. M. Ramos, I. M. Fonseca and J. Vital, New method for the immobilization of nitroxyl radical on mesoporous silica, *Microporous Mesoporous Mater.*, 2015, **203**, 63–72.

16 B. Karimi, E. Farhangi, H. Vali and S. Vahdati, SBA-15-Functionalized 3-Oxo-ABNO as Recyclable Catalyst for Aerobic Oxidation of Alcohols under Metal-Free Conditions, *ChemSusChem*, 2014, **7**, 2735–2741.

17 Z. Zheng, J. Wang, M. Zhang, L. Xu and J. Ji, Magnetic Polystyrene Nanosphere Immobilized TEMPO: A Readily Prepared, Highly Reactive and Recyclable Polymer Catalyst in the Selective Oxidation of Alcohols, *ChemCatChem*, 2013, **5**, 307–312.

18 S. Campestrini, C. Corvaja, M. De Nardi, C. Ducati, L. Franco, M. Maggini, M. Meneghetti, E. Menna and G. Ruaro, Investigation of the Inner Environment of Carbon Nanotubes with a Fullerene-Nitroxide Probe, *Small*, 2008, **4**, 350–356.

19 C. Aprile, F. Giacalone, M. Gruttadauria, A. M. Marculescu, R. Noto, J. D. Revell and H. Wennemers, New ionic liquid-modified silica gels as recyclable materials for l-proline- or H–Pro–Pro–Asp–NH_2-catalyzed aldol reaction, *Green Chem.*, 2007, **9**, 1328.

20 P. L. Anelli, C. Biffi, F. Montanari and S. Quici, Fast and selective oxidation of primary alcohols to aldehydes or to carboxylic acids and of secondary alcohols to ketones mediated by oxoammonium salts under two-phase conditions, *J. Org. Chem.*, 1987, **52**, 2559–2562.
21 P. Naik, J. García-Lacuna, P. O'Neill and M. Baumann, Continuous Flow Oxidation of Alcohols Using TEMPO/NaOCl for the Selective and Scalable Synthesis of Aldehydes, *Org. Process Res. Dev.*, 2024, **28**, 1587–1596.
22 Y. Zhao, Y. Kondo, Y. Kuwahara, K. Mori and H. Yamashita, Two-phase reaction system for efficient photocatalytic production of hydrogen peroxide, *Appl. Catal., B*, 2024, **351**, 123945.
23 Y. Isaka, Y. Kawase, Y. Kuwahara, K. Mori and H. Yamashita, Two-Phase System Utilizing Hydrophobic Metal–Organic Frameworks (MOFs) for Photocatalytic Synthesis of Hydrogen Peroxide, *Angew. Chem.*, 2019, **131**, 5456–5460.
24 Y. Nakamura, M. Linden, J. Winter, S. Hofmann, N. Shida, M. Atobe and S. R. Waldvogel, Biphasic Electrosynthesis of 2-Isoxazol(in)e-3-carboxylates: Reaction Optimization from Milligram to Hectogram Scale, *ACS Sustainable Chem. Eng.*, 2024, **12**, 11369–11376.
25 G. Zhao, T. Jiang, W. Wu, B. Han, Z. Liu and H. Gao, Electro-oxidation of Benzyl Alcohol in a Biphasic System Consisting of Supercritical CO_2 and Ionic Liquids, *J. Phys. Chem. B*, 2004, **108**, 13052–13057.
26 Z. Li, Y. Yan, S.-M. Xu, H. Zhou, M. Xu, L. Ma, M. Shao, X. Kong, B. Wang, L. Zheng and H. Duan, Alcohols electrooxidation coupled with H_2 production at high current densities promoted by a cooperative catalyst, *Nat. Commun.*, 2022, **13**, 147.
27 R. Shi, X. Zhang, C. Li, Y. Zhao, R. Li, G. I. N. Waterhouse and T. Zhang, Electrochemical oxidation of concentrated benzyl alcohol to high-purity benzaldehyde via superwetting organic-solid-water interfaces, *Sci. Adv.*, 2024, **10**, eadn0947.
28 L. Ni, C. Yu, Q. Wei, D. Liu and J. Qiu, Pickering Emulsion Catalysis: Interfacial Chemistry, Catalyst Design, Challenges, and Perspectives, *Angew. Chem., Int. Ed.*, 2022, **61**, e202115885.
29 S. Crossley, J. Faria, M. Shen and D. E. Resasco, Solid Nanoparticles that Catalyze Biofuel Upgrade Reactions at the Water/Oil Interface, *Science*, 2010, **327**, 68–72.
30 F. Zhang, Q.-Y. Fan, Y.-C. Huang, H. Li, H. Zou, Y. Li, Y. Zou, S. Wang, C. Yang, Y. Lu and H. Yang, A Pickering-emulsion-droplet-integrated electrode for the continuous-flow electrosynthesis of oximes, *Nat. Synth.*, 2025, **4**, 479–487.
31 E. Piacentini, R. Mazzei and L. Giorno, Comparison between Lipase Performance Distributed at the O/W Interface by Membrane Emulsification and by Mechanical Stirring, *Membranes*, 2021, **11**, 137.
32 H. Gröger, O. May, H. Hüsken, S. Georgeon, K. Drauz and K. Landfester, Enantioselective Enzymatic Reactions in Miniemulsions as Efficient 'Nanoreactors', *Angew. Chem., Int. Ed.*, 2006, **45**, 1645–1648.
33 D. Meroni, C. Cionti, G. Vavassori, D. Maggioni and G. Cappelletti, Multistimuli Responsive ZnO-Stabilized Pickering Emulsions for the Controlled Release of Essential Oils, *ACS Sustainable Chem. Eng.*, 2025, **13**, 482–493.
34 M. Cai, S. Dai, J. Xuan and Y. Mo, Bromide-mediated membraneless electrosynthesis of ethylene carbonate from CO_2 and ethylene, *Nat. Commun.*, 2025, **16**, 3285.
35 K. M. Lee, J. H. Jang, M. Balamurugan, J. E. Kim, Y. I. Jo and K. T. Nam, Redox-neutral electrochemical conversion of CO_2 to dimethyl carbonate, *Nat. Energy*, 2021, **6**, 733–741.
36 Y. Zhang, A. Iqbal, J. Zai, S.-Y. Zhang, H. Guo, X. Liu, I. ul Islam, H. Fazal and X. Qian, Bromine and oxygen redox species mediated highly selective electro-epoxidation of styrene, *Org. Chem. Front.*, 2022, **9**, 436–444.
37 F. Struyven, M. Sellier and P. Mandin, Review: Interactions between electrogenerated bubbles and microfluidic phenomena, *Int. J. Hydrogen Energy*, 2023, **48**, 32607–32630.
38 Y. Dai, C. F. Chamberlayne, M. S. Messina, C. J. Chang, R. N. Zare, L. You and A. Chilkoti, Interface of biomolecular condensates modulates redox reactions, *Chem*, 2023, **9**, 1594–1609.
39 K. Piradashvili, E. M. Alexandrino, F. R. Wurm and K. Landfester, Reactions and Polymerizations at the Liquid–Liquid Interface, *Chem. Rev.*, 2016, **116**, 2141–2169.
40 P. Cintas, Ultrasound and green chemistry – Further comments, *Ultrason. Sonochem.*, 2016, **28**, 257–258.
41 J. L. Rodríguez and E. Pastor, A comparative study on the adsorption of benzyl alcohol, toluene and benzene on platinum, *Electrochim. Acta*, 2000, **45**, 4279–4289.
42 H. Huang, X. Song, C. Yu, Q. Wei, L. Ni, X. Han, H. Huang, Y. Han and J. Qiu, A Liquid-Liquid-Solid System to Manipulate the Cascade Reaction for Highly Selective Electrosynthesis of Aldehyde, *Angew. Chem., Int. Ed.*, 2023, **62**, e202216321.
43 J. M. Hoover, B. L. Ryland and S. S. Stahl, Mechanism of Copper(I)/TEMPO-Catalyzed Aerobic Alcohol Oxidation, *J. Am. Chem. Soc.*, 2013, **135**, 2357–2367.
44 M. Zhao, J. Li, E. Mano, Z. Song, D. M. Tschaen, E. J. J. Grabowski and P. J. Reider, Oxidation of Primary Alcohols to Carboxylic Acids with Sodium Chlorite Catalyzed by TEMPO and Bleach, *J. Org. Chem.*, 1999, **64**, 2564–2566.
45 H. Zhang, L. Fu and H. Zhong, Silica gel-supported TEMPO with adsorbed NOx for selective oxidation of alcohols under mild conditions, *Chin. J. Catal.*, 2013, **34**, 1848–1854.
46 T. Fey, H. Fischer, S. Bachmann, K. Albert and C. Bolm, Silica-Supported TEMPO Catalysts: Synthesis and Application in the Anelli Oxidation of Alcohols, *J. Org. Chem.*, 2001, **66**, 8154–8159.
47 Y. Hase, E. Ito, T. Shiga, F. Mizuno, H. Nishikoori, H. Iba and K. Takechi, Quantitation of Li_2O_2 stored in Li–O_2 batteries based on its reaction with an oxoammonium salt, *Chem. Commun.*, 2013, **49**, 8389.
48 M. Thommes, K. Kaneko, A. V. Neimark, J. P. Olivier, F. Rodriguez-Reinoso, J. Rouquerol and K. S. W. Sing, Physisorption of gases, with special reference to the evaluation of surface area and pore size distribution (IUPAC Technical Report), *Pure Appl. Chem.*, 2015, **87**, 1051–1069.

49 M. Thommes, Physical Adsorption Characterization of Nanoporous Materials, *Chem. Ing. Tech.*, 2010, **82**, 1059–1073.
50 K. S. W. Sing, Reporting physisorption data for gas/solid systems with special reference to the determination of surface area and porosity, *Pure Appl. Chem.*, 1982, **54**, 2201–2218.
51 T. Raju, S. Manivasagan, B. Revathy, K. Kulangiappar and A. Muthukumaran, A mild and efficient method for the oxidation of benzylic alcohols by two-phase electrolysis, *Tetrahedron Lett.*, 2007, **48**, 3681–3684.
52 A. J. Bosco, S. Lawrence, C. Christopher, S. Radhakrishnan, A. A. Joseph Rosario, S. Raja and D. Vasudevan, Redox-mediated oxidation of alcohols using Cl^-/OCl^- redox couple in biphasic media, *J. Phys. Org. Chem.*, 2015, **28**, 591–595.
53 T. Inokuchi, S. Matsumoto and S. Torii, Indirect electrooxidation of alcohols by a double mediatory system with two redox couples of $[R_2N^+{=}O]/R_2NO\cdot$ and $[Br\cdot$ or $Br^+]/Br^-$ in an organic-aqueous two-phase solution, *J. Org. Chem.*, 1991, **56**, 2416–2421.
54 Y. Chen, S. Wang, Z. Xu, Y. Wang, J. He, K. Li, J. Wang, L. Liu, L. Ren, S. Li, Z. Zhang, X. Zhong and J. Wang, Boosting electrocatalytic alcohol oxidation: Efficient d–π interaction with modified TEMPO and bioinspired structure, *AIChE J.*, 2025, **71**, e18662.
55 C. Li, X. Li, X. Du, T. Tong, T. Y. Cath and J. Lee, Antiwetting and Antifouling Janus Membrane for Desalination of Saline Oily Wastewater by Membrane Distillation, *ACS Appl. Mater. Interfaces*, 2019, **11**, 18456–18465.
56 N. Naimah, N. N. R. Agmad, A. W. Lun and L. C. Peng, Current advances in membrane technologies for saline wastewater treatment: A comprehensive review, *Desalination*, 2021, **517**, 115170.
57 Z. Yan, X. Chen, H. Chang, H. Pang, G. Fan, K. Xu, H. Liang and F. Qu, Feasibility of replacing proton exchange membranes with pressure-driven membranes in membrane electrochemical reactors for high salinity organic wastewater treatment, *Water Res.*, 2024, **254**, 121340.
58 H. Chang, Y. Zhu, L. Huang, Z. Yan, F. Qu and H. Liang, Mineral scaling induced membrane wetting in membrane distillation for water treatment: Fundamental mechanism and mitigation strategies, *Water Res.*, 2023, **247**, 120807.
59 H. Zhu, M. Cai, X. Wang and L. Dai, Highly efficient electro-epoxidation of olefins coupled with bromine recycling, *Green Chem.*, 2025, **27**, 5366–5375.
60 J. Luo, C. Zhang, W. Liu, Y. Li, B. Xie and J. Zhang, Synthesis of a sustainable and robust heterogeneous TEMPO catalyst utilizing activated carbon for aerobic alcohol oxidation, *React. Chem. Eng.*, 2024, **9**, 1444–1451.
61 J. Luo, TEMPO immobilization on activated carbon by a novel surface-formylation tactic for long-term aerobic oxidation of alcohols, *Chem. Eng. J.*, 2023, **471**, 144454.
62 A. Dijksman, A. Marino-González, A. M. I. Payeras, I. W. C. E. Arends and R. A. Sheldon, Efficient and Selective Aerobic Oxidation of Alcohols into Aldehydes and Ketones Using Ruthenium/TEMPO as the Catalytic System, *J. Am. Chem. Soc.*, 2001, **123**, 6826–6833.
63 S. A. Tromp, I. Matijošytė, R. A. Sheldon, I. W. C. E. Arends, G. Mul, M. T. Kreutzer, J. A. Moulijn and S. de Vries, Mechanism of Laccase–TEMPO-Catalyzed Oxidation of Benzyl Alcohol, *ChemCatChem*, 2010, **2**, 827–833.
64 M. Suleiman, M. Sankaranarayanan, K. Theva Das, S. I. Amran, V. Berezin, B. Andrey and J. Jamalis, Vanillin Derivatives in Drug Design: Structure–Activity Relationship (SAR) Hotspots and Synthetic Pathways for Enhanced Pharmacological Activity, *ACS Omega*, 2025, **10**, 57846–57875.

